Supporting Information

Textured Microcapsules through Crystallization

*Samuel R. Wilson-Whitford,[‡,†] Ross W. Jaggers,[‡] Brooke W. Longbottom,[‡,§] Matt K. Donald,[‡] Guy J. Clarkson,[‡] and Stefan A. F. Bon.[‡,]**

‡Samuel R. Wilson-Whitford, Ross W. Jaggers, Brooke W. Longbottom, Matt K. Donald, Guy J. Clarkson, and Stefan, A. F. Bon, Department of Chemistry, University of Warwick, Gibbet Hill Road, Coventry, CV4 7AL, United Kingdom.

†Samuel R. Wilson-Whitford, Department of Chemical and Biomolecular Engineering, Lehigh University, 19 Memorial Drive W., Bethlehem, Pennsylvania, 18015-3027, USA.

§Brooke W. Longbottom, Department of Chemistry, University of Cambridge, Lensfied Road, Cambridge, CB2 1EW, United Kingdom.

*Stefan A. F. Bon, E-Mail: s.bon@warwick.ac.uk

Decane-1,10-bis(cyclohexyl carbamate) (DBCC) characterization

^{1}H NMR (400 MHz, $CDCl_3$, δ): = 4.47 (s, 2H, NH(C=O)), 3.95 (t, ^{3}J = 5.8 Hz, 4H, OCH_2), 3.40 (s, 2H, CH), 1.87-1.06 (m, 36H, Ar H + CH_2). ^{13}C NMR (400 MHz, $CDCl_3$, δ): = 158.01 (C=O), 64.74 (CH_2), 49.69 (CH), 33.49 (CH_2), 29.42 (CH_2), 29.25 (CH_2), 29.06 (CH_2), 25.87 (CH_2), 25.52 (CH_2), 24.81 (CH_2). IR(KBr): ν = 3337 (s; (NH)), 2918 (s; $\nu_{as}(CH_2)$), 2851(s; $\nu_{s}(CH_2)$), 1678 (s; (C=O)), 1527 (b; (NH)), 1225 (s; (C-N)), 1042 (s; (C-O)), 630 (b; (CH)). HRMS (ESI) *m/z*: $[M+Na]^+$ calcd for $C_{24}H_{44}N_2O_4Na$, 447.3198; found, 447.3193.

A suitable crystal of DBCC was selected and mounted on a Mitegen head with Fromblin oil and placed on an Xcalibur Gemini diffractometer with a Ruby CCD area detector. The crystal was kept at 295(1) K during data collection. Using Olex2,[1] the structure was solved with the ShelXT structure solution program using Direct Methods and refined with the ShelXL refinement package using Least Squares minimisation.[2,3]

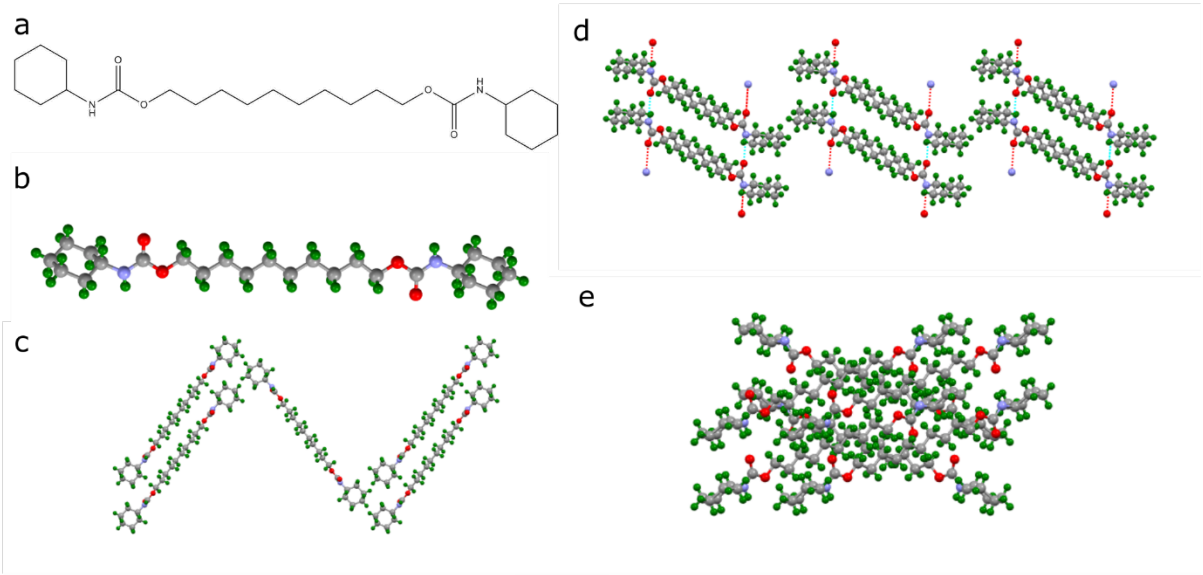

Figure S1. *(a)* Molecular structure of decane-1,10-bis(cyclohexyl carbamate) (DBCC) *(b)* Crystallographic structure of DBCC *(c)* Crystal structure of DBCC down a-axis of the lattice *(d)* down b-axis *(e)* down c-axis.

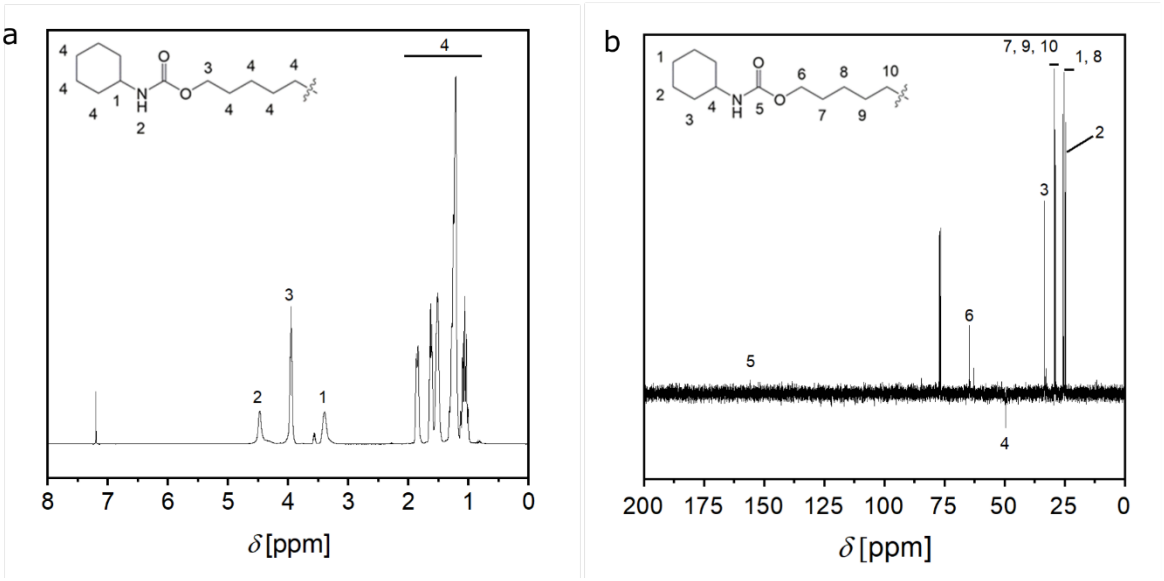

Figure S2. *(a)* $CDCl_3$ ^1H NMR of decane-1,10-diyl bis(cyclohexylcarbamate) (*b*) $CDCl_3$ ^{13}C NMR of decane-1,10-diyl bis(cyclohexylcarbamate).

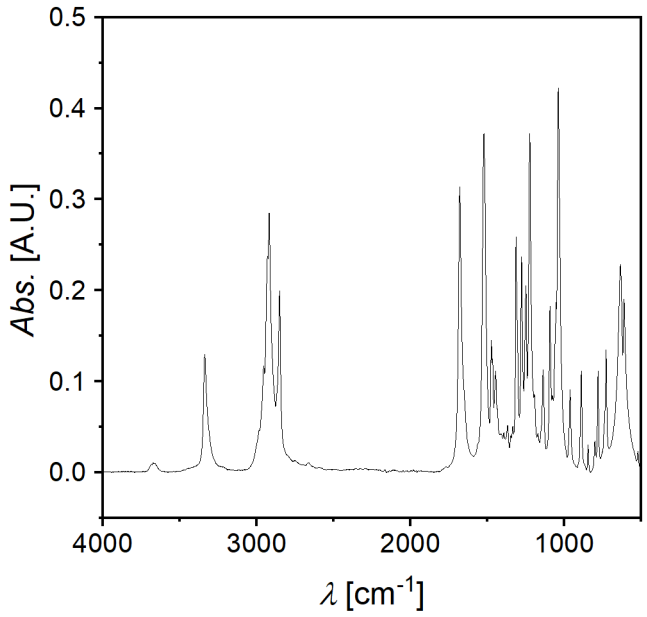

Figure S3. FTIR spectra of decane-1,10-diyl bis(cyclohexylcarbamate).

Organogelation

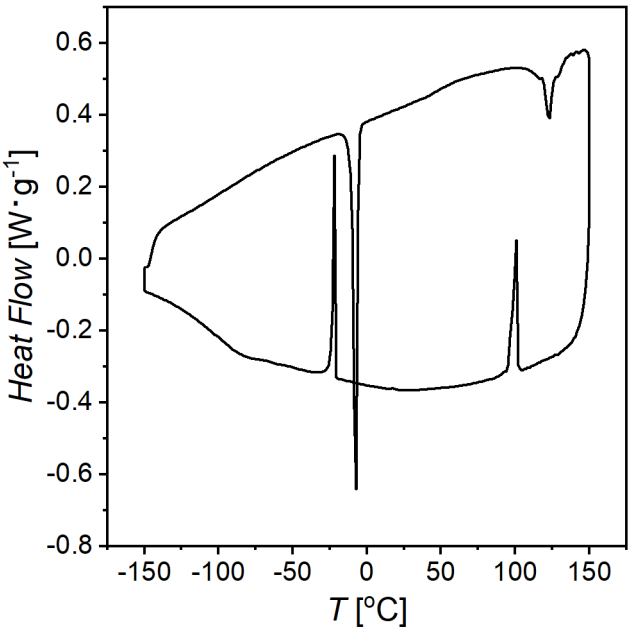

Figure S4. Differential scanning calorimetry of 5 wt.% DBCC organogel in dodecane.

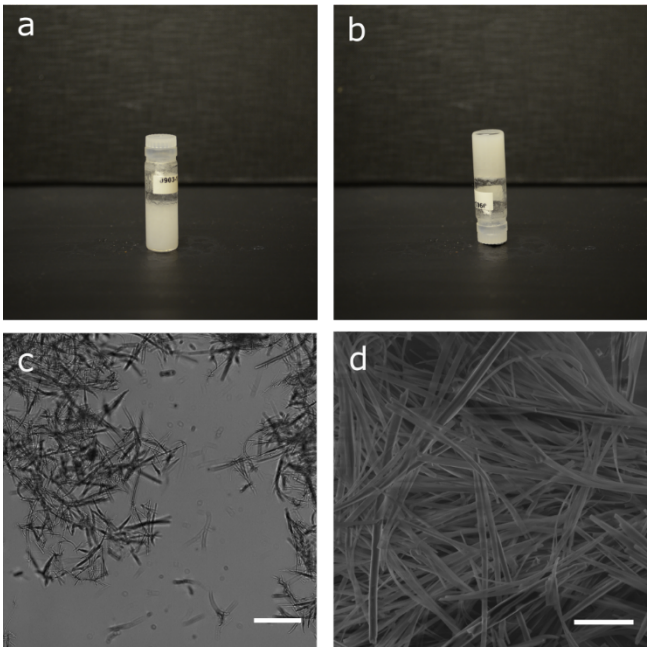

Figure S5. Inversion tests of organogels *(a)* 1 wt.% DBCC in dodecane *(b)* inversion of DBCC in dodecane *(c)* 20 x light microscopy of 1 wt. % DBCC in dodecane *(d)* SEM 1 wt. % DBCC in dodecane.

Microfluidics

Description of device assembly and materials in work of Bon[4].

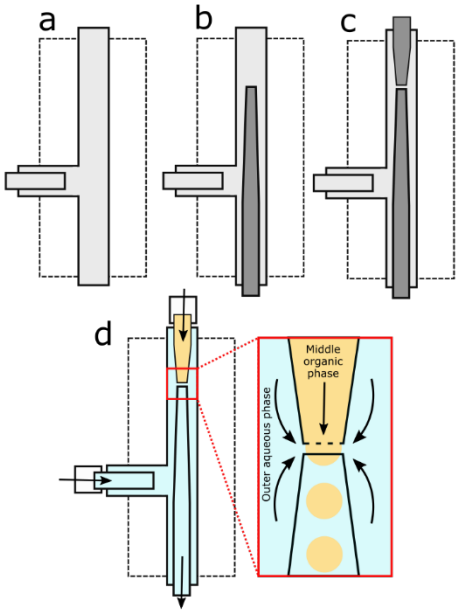

Figure S6. *(a-c)* Construction of glass microfluidic device *(d)* experimental operation of glass microfluidic device.

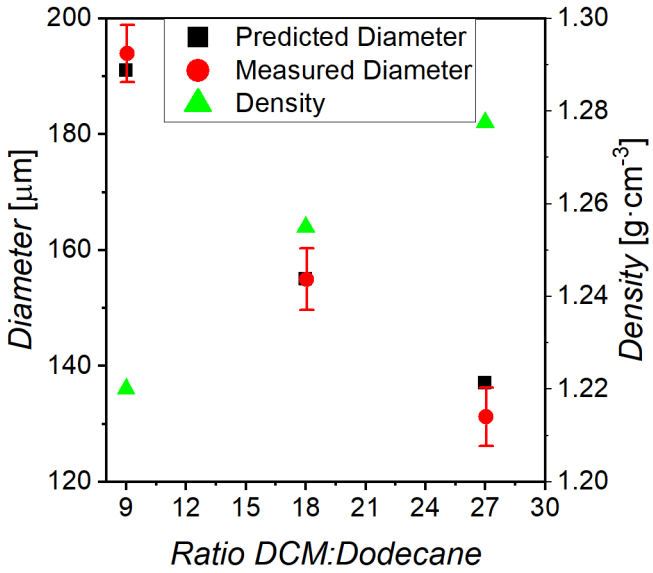

Figure S7. Plot of predicted capsule size (black squares) against measured capsule size (red circles) when generated with different DCM:dodecane ratios 9:1, 18:1 and 27:1. Also shown, density of DCM:dodecane blends (green triangles).

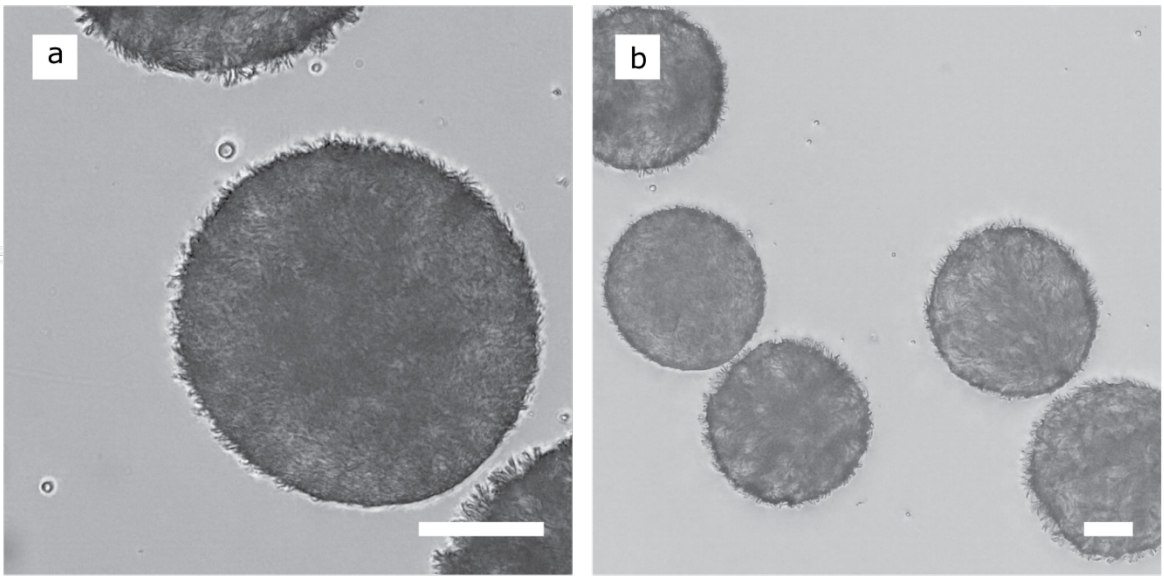

Figure S8. Light microscopy of textured surface of microcapsules generated by microfluidics *(a)* Scale bar = 100 µm *(b)* Scale bar = 50 µm.

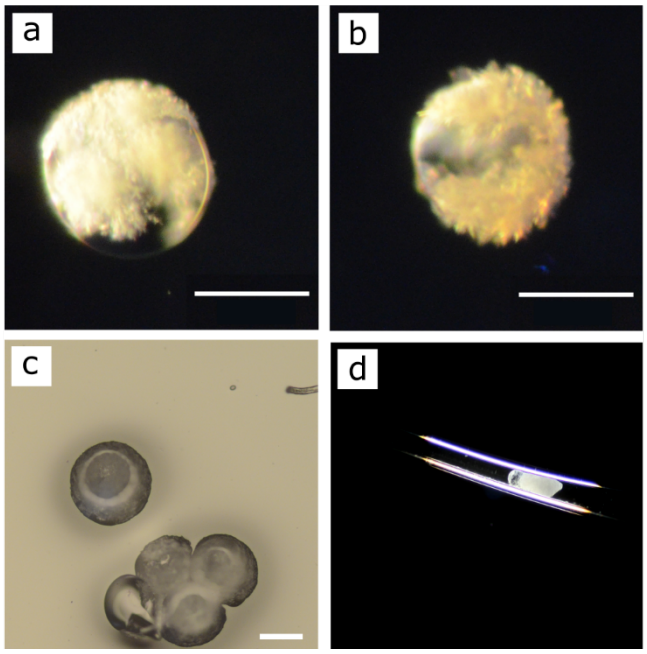

Figure S9. *(a)* Image of incomplete capsule coverage from satellite droplet *(b)* Image of incomplete capsule coverage from satellite droplet *(c)* Dried capsule imaged with back scattering showing collapsed capsule structure following dodecane evaporation. *(d)* Capsule pushed through narrow capillary to force out central droplet. Scale Bar = 100 µm.

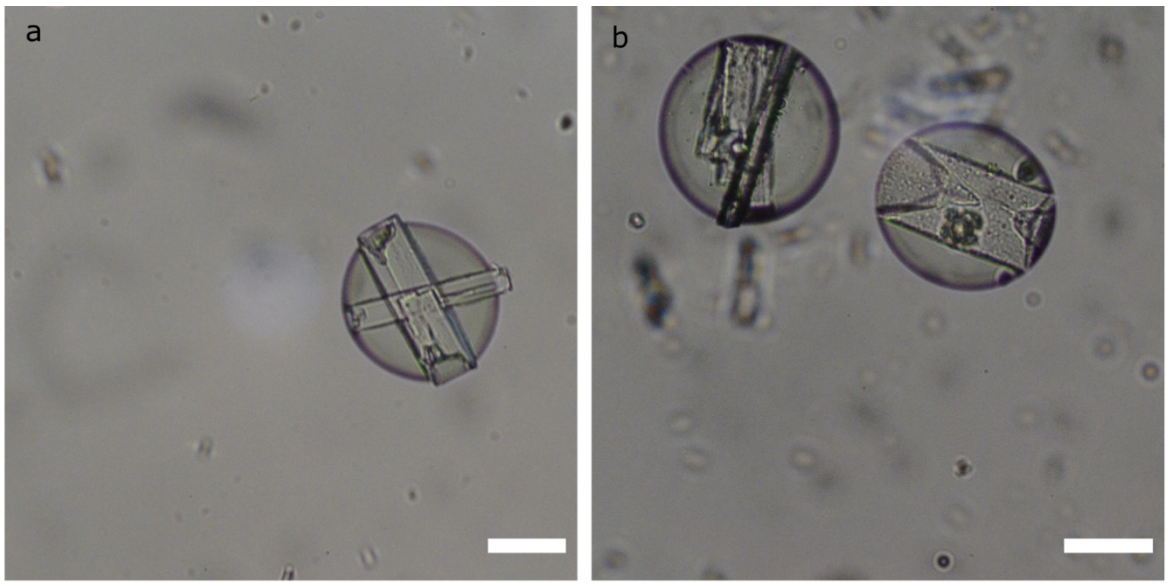

Figure S10. *(a-b)* Bright-field microscopy of single crystals growing inside droplets when particulates nucleate crystal growth heterogeneously. Scale Bar = 100 µm.

Shell Thickness

Nile Red was visualised using a white light laser (λ =495 nm, 30 % intensity) with a spectral detection window of 484 – 499 nm for reflected light and 584nm - 704nm for fluorescent light. Data was collected and analysed using the Leica LAS-AF confocal acquisition software.

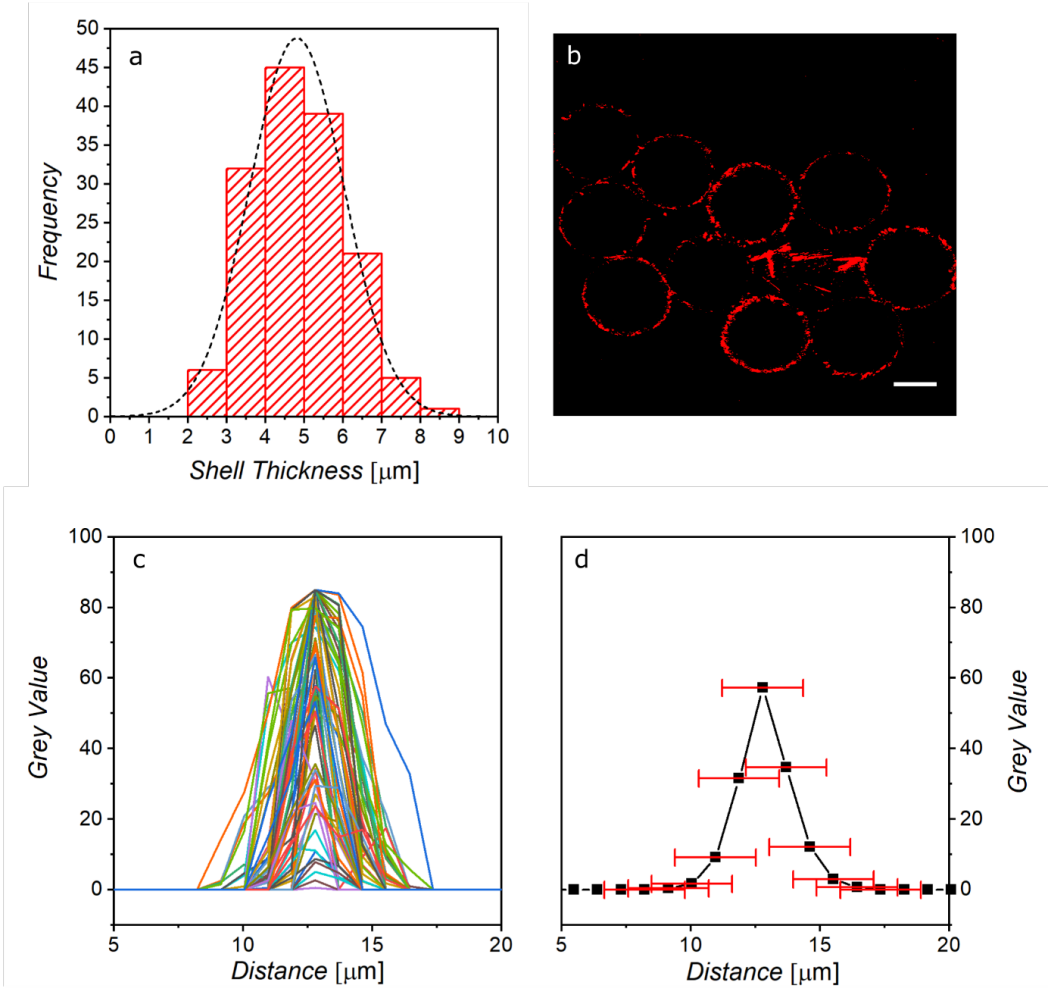

Figure S11. *(a)* Histogram of 149 shell thickness measurements made manually. Resulting average thickness = 4.81 ± 1.21 µm. *(b)* Thresholded reflectance confocal image of 220 µm capsules focus at capsule volume centre. Scale bar = 100 µm *(c)* 62 x-axis shifted intensity profiles of thresholded confocal image *(d)* Average intensity profile across capsule wall and associated error. Resulting average thickness = 5.72 ± 1.56 µm.

Small Capsules

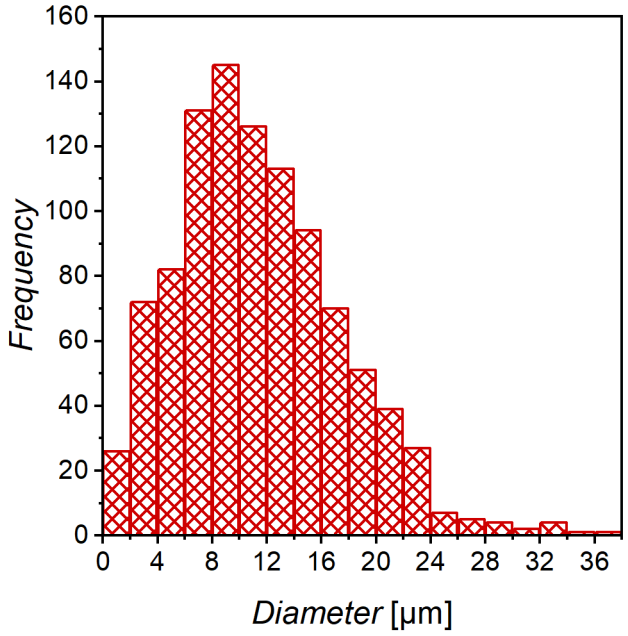

Figure S12. Size distribution of spikey capsules synthesised at 1000 rpm via the batch synthesis.

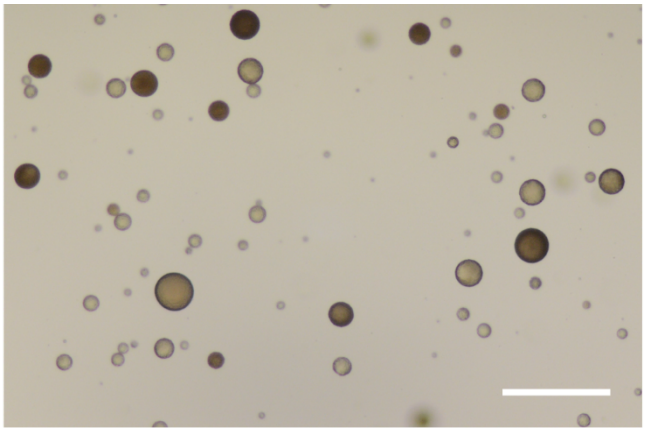

Figure S13. 1:1 blend of smooth (light brown) and rough (dark brown) small microcapsules images with a light microscope in back scattering mode. Scale bar = 100 µm.

Scanning electron microscopy imaging

Capsules for SEM analysis contained hexamethylenediacrylate in place of dodecane. A photoinitiator, phenylbis(2,4,6-trimethyl-benzoyl)phospine oxide, was also added to allow rapid UV curing.

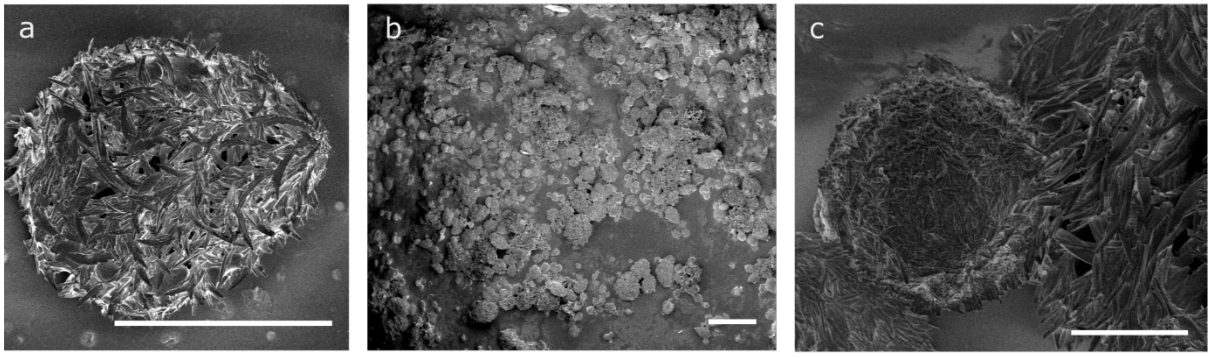

Figure S14. Scanning electron micrograph of acrylate crosslinked DBCC capsules. *(a)* Synthesised by microfluidics. Scale bar = 100 μm *(b)* Synthesised in batch. Scale bar = 100 μm *(c)* Comparison of crystal size between large capsule and smaller 40 μm capsule. Scale bar = 20 μm.

Surface Roughness

Surface roughness measurements were calculated from light microscopy using a radial surface profile imageJ plugin – radialSurfProfile available free of charge from github user blongbot. https://github.com/blongbot/radialSurfProfile.

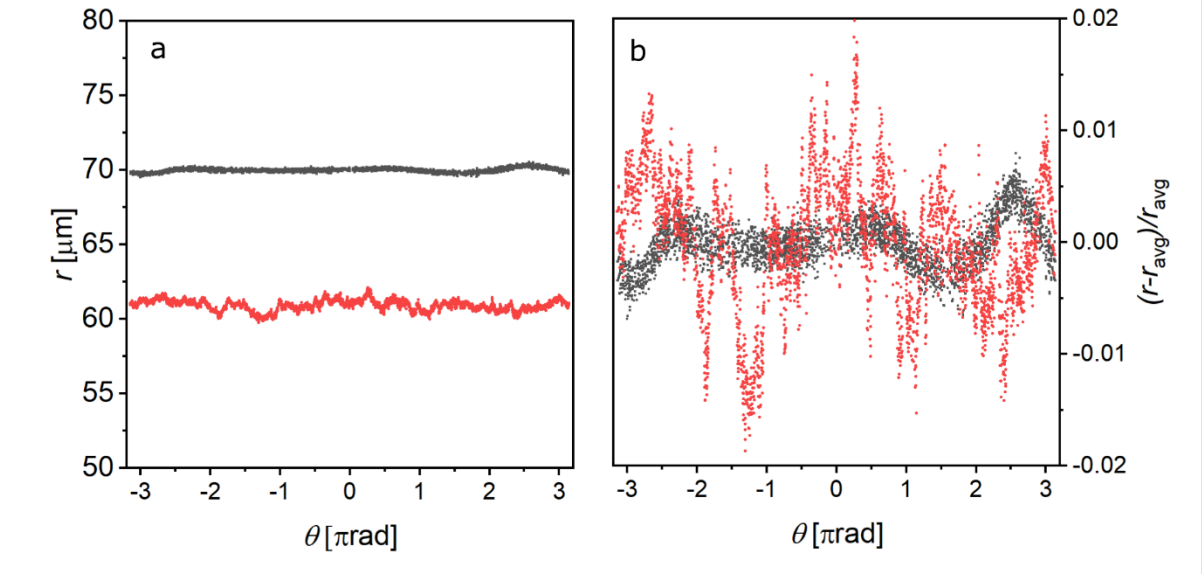

Figure S15. *(a)* Comparison of capsule roughness in smooth (black) and spikey (red) capsules measured as a radius from centre of mass of the capsule for each radial increment. *(b)* Average radius normalized surface roughness of smooth (black) and spikey (red) capsules. Capsules produced by batch method.

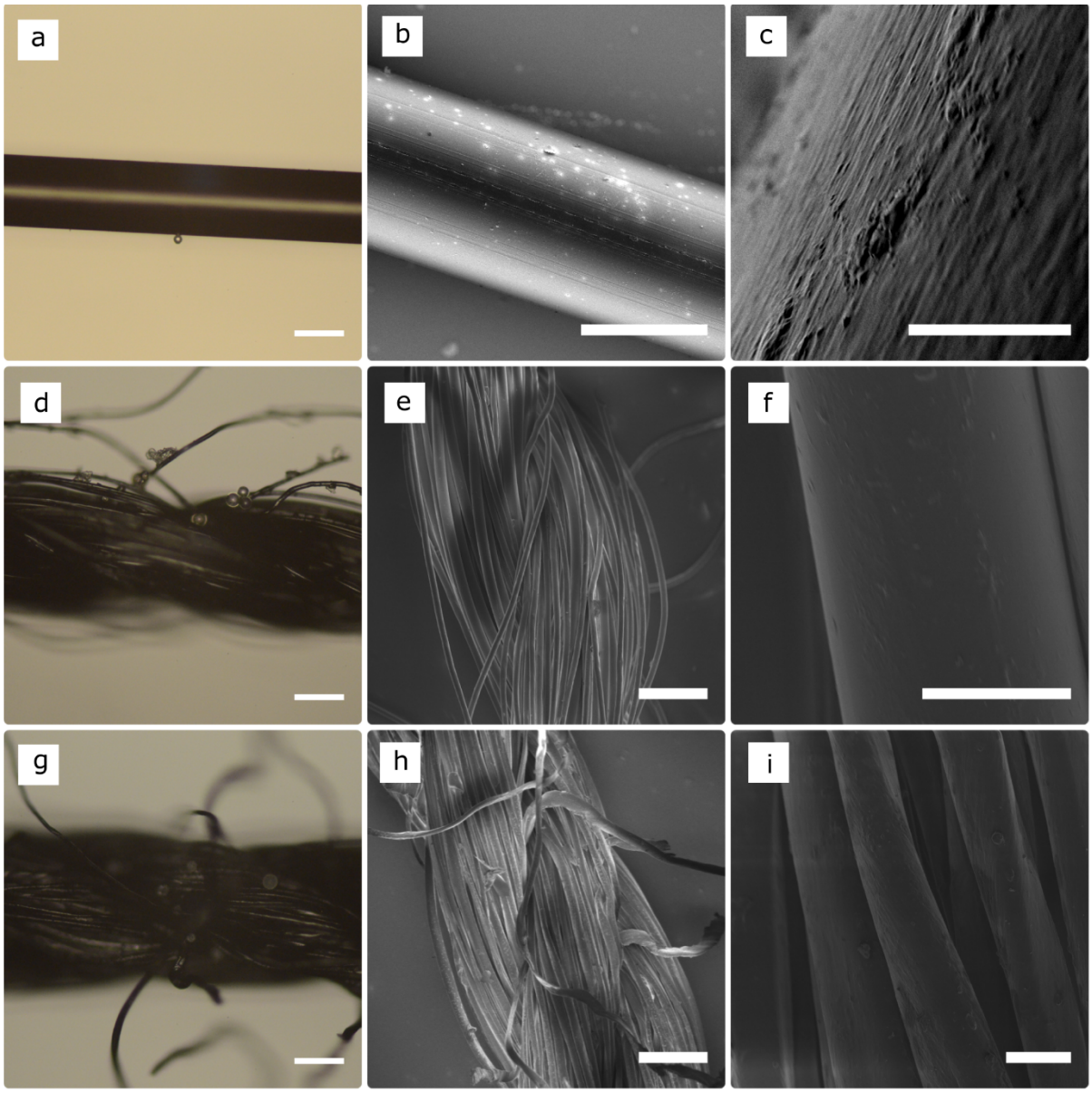

Figure S16. *(a)* Backscatter light microscopy of polyamide fibre with adhered capsule. Scale: 100 µm *(b-c)* SEM microscopy of polyamide. Scale: 100 µm and 5 µm *(d)* Backscatter light microscopy of polyester fibre with adhered capsules. Scale: 100 µm *(e-f)* SEM microscopy of polyester. Scale: 100 µm and 10 µm *(g)* Backscatter light microscopy of cotton fibre with adhered capsules. Scale: 100 µm *(h-i)* SEM microscopy of cotton. Scale: 100 µm and 10 µm.

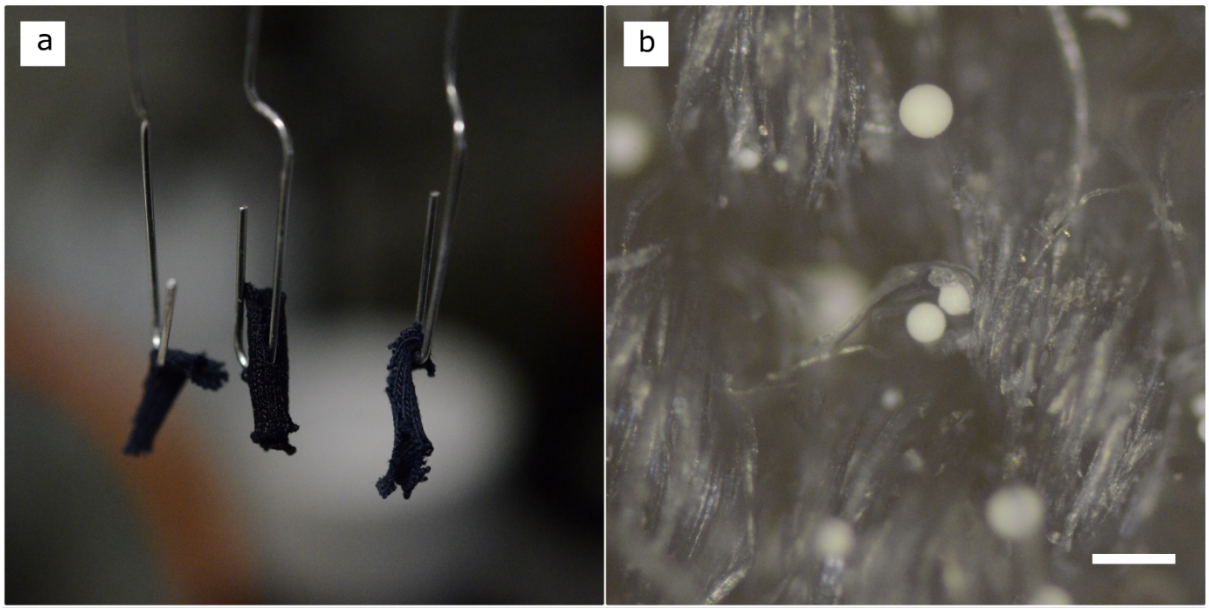

Figure S17. *(a)* Photograph of drying 100 mm^2 cotton squares following dipping *(b)* 1 mm^2 quadrant of dried cotton square viewed by backscattered light microscopy.

References

(1) Dolomanov, O. V.; Bourhis, L. J.; Gildea, R. J.; Howard, J. A. K.; Puschmann, H. OLEX2: A Complete Structure Solution, Refinement and Analysis Program. *J. Appl. Crystallogr.* **2009**, *42* (2), 339–341.

(2) Sheldrick, D. M. SHELXT - Integrated Space-Group and Crystal-Structure Determination. *Acta Crystallogr.* **2015**, *A71*, 3–8.

(3) Sheldrick, D. M. Crystal Structure Refinement with SHELXL. *Acta Crystallogr.* **2015**, *C71*, 3–8.

(4) Jaggers, R. W.; Bon, S. A. F. Independent Responsive Behaviour and Communication in Hydrogel Objects. *Mater. Horizons* **2017**, *4* (3), 402–407.